ACS OMEGA

http://pubs.acs.org/journal/acsodf

Article

Banana Peel Waste: An Emerging Cellulosic Material to Extract Nanocrystalline Cellulose

Shweta Mishra, Bala Prabhakar,* Prashant S. Kharkar, and Anil M. Pethe

Cite This: *ACS Omega* 2023, 8, 1140−1145

Read Online

ACCESS | Metrics & More | Article Recommendations

ABSTRACT: Nanocrystalline cellulose (NCC) has gained attention due to its versatile properties such as biocompatibility, sustainability, high aspect ratio, and abundance of −OH groups that favor modifications of NCC. The objective of this paper is to develop NCC by extracting and characterizing NCC prepared from banana peel powder (BPP). BPP was subjected to alkali and bleaching treatment to remove lignin and hemicellulose and then subjected to acid hydrolysis to prepare NCC. Under optimal conditions (200 mL of sulfuric acid 55% v/v at 50 °C for 60 min), the NCC yield was found to be 29.9%. The particle size and zeta potential of the NCC were found to be 209 nm and −43 mV, respectively. Attenuated total reflectance Fourier transform infrared spectroscopy showed successful removal of lignin and hemicellulose from BPP after the alkali treatment, bleaching, and acid hydrolysis. Field emission scanning electron microscopy showed needle-shaped crystals and transmission electron microscopy showed particles in the nano range. X-ray diffraction analysis showed that the crystallinity index of NCC was 64.12% while keeping the cellulose I crystal structure intact. Thermogravimetric analysis showed good stability which paves way for NCC to be explored for various applications. All the parameters evaluated indicated that NCC was successfully prepared from BPP using alkali treatment, bleaching, and acid hydrolysis.

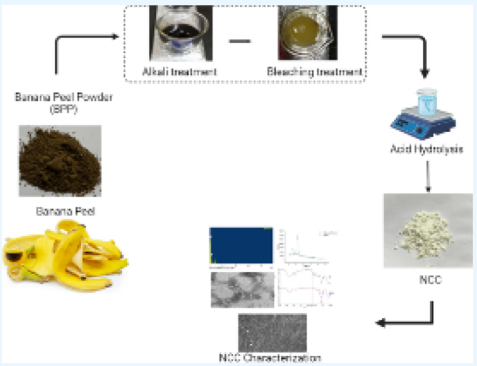

1. INTRODUCTION

India has a very diverse agro climate which encourages the cultivation of numerous crops including medicinal herbs, ornamental plants, decorative plants, vegetables, trees, roots tubers, spices, and plantation crops. India is the second-largest producer of fruits and vegetables, in the world. Lignocellulosic biomass is produced on large scale every year during harvesting, cultivation processing, and consumption of agricultural products[1,2]

Banana is the most widely used fruit worldwide for several good reasons, as it is a delicious, rich source of nutrients and also helps in improving mental health.[3] Banana (*Musa* sp., family Musaceae) develops in hanging clusters with an average fruit weight of about 125 g with nearly 25% dry matter and 75% water. Banana is the second largest produced fruit accounting for 16% of the total fruit production worldwide. In 2019, worldwide approximately 119 million tons of bananas were produced. Among that, India is the world's biggest banana producer with 31.50 million tons of production.[2] Lot of production and consumption comes with a lot of waste production comprising 30−40% of total weight resulting approximately 3.5 million tons of banana peel (BP) waste per year.[4,5] Banana is extensively used by various food, juice, cosmetic, and textile industries.[6,7]

BP comprises about 60−70% (w/w) of carbohydrate, protein (2−3%), fiber (4−5%), lipid (4−5%), and moisture (20%).[8] However, on dry basis, BP contains 7.6−9.6% cellulose, 10−21% pectin, 6.4−9.4% hemicellulose, 6−12% lignin, and some low molecular compounds on dry basis.[4] BP as a waste takes up to 2 years to decompose and biodegrade as it contains carbon-rich organic compounds. This produces excessive emissions of greenhouse gases that contribute to climate change. Huge quantity of BP waste is produced by various industries and fruit markets which is either considered as agricultural waste and left to rot in farms to provide nutrients to the soil or just discarded as a waste product.

In some places, agricultural waste burning is practiced and considered the most effective and efficient way of clearing landfills. This fire is the largest source of carbon black which is a threat to environment and humans.[9] This waste can be converted into useful materials instead of being dumped in landfills, and reduce environmental and economic problems.[10−12] The utilization of agricultural waste would help in improving the environment by reducing toxic emissions and carbon black. Currently, researchers are focusing on the utilization of agricultural waste for various biomedical and

Received: October 12, 2022
Accepted: November 30, 2022
Published: December 28, 2022

© 2022 The Authors. Published by American Chemical Society

pharmaceutical purposes which are the need of the hour to protect planet earth from extensive climate change and the damage caused by it. In the last 2 decades, a lot of work has been reported about utilizing agricultural waste in the best possible way. Faradilla et al. prepared nanocellulose from banana pseudo-stem by TEMPO-mediated oxidation. The results showed that prepared nanocellulose is more crystalline than pseudo-stem.[13] Harini et al. used BP and banana bract for the preparation of nanocellulose fibers (CNFs) by the microwave digestion method and ball milling-assisted ultrasonication method. The extracted CNFs were used for the production of cellulose-based biopolymers through acetyl and lauroyl modifications.[14] Sijabat et al. prepared a flat sheet membrane composite using bacterial nanocellulose (derived from BP waste, cellulose, and silica). The prepared sheet was used for the desalination process and the results showed optimal performance.[15] Din et al. used unripe BP for the development of cellulose nanofibers which was later used for the development of a bio-based nanocomposite packaging film. The result showed that these films have good tensile strength and could be used for food packaging due to their properties such as biocompatibility, biodegradability, and non-toxicity.[16,17]

Agricultural waste is commonly used for developing nanocrystalline cellulose (NCC) and then functionalized by various modifications. To date, NCC has been explored for various biomedical applications. It is used for enzyme immobilization, in wound dressing, tissue engineering, bio sensing, bio imaging, and for drug delivery.[18] Apart from medical uses, it is also used for waste water management, as a packaging material, in supercapacitors and conductive films. NCC also works as a rheological modifier, Pickering emulsion stabilizer and in free radical scavenging.[19,20] Conversion of agricultural waste into NCC opens a lot of ways for utilization of waste in the best possible manner. This study aims to prepare NCC from BP powder (BPP) by alkali and bleaching treatment, followed by acid hydrolysis.

2. MATERIALS AND METHODS

2.1. Materials. The BP used for the preparation were collected from the local juice center and fruit sellers from Vile Parle West, Mumbai, India. The collected BP were cut into small pieces. Dewaxing of small pieces of BP was carried out by using Soxhlet extraction with acetone as the solvent. After the treatment, BP were dried at room temperature for 6 h and then kept in the oven at 50 °C for 1 week. Dried peels were collected and pulverized by using a cutter mill and jet mill. The powder was termed BPP and stored for future use. The average particle size of BPP was approx. 10−15 μ.

Sodium hydroxide was used for alkali treatment. Sodium hypochlorite was used as the bleaching agent and sulfuric acid was used for acid hydrolysis. Analytical grade sodium hydroxide, sodium hypochlorite, and sulfuric acid were procured from Research-lab Chemical Corporation. The dialysis tube having a molecular cut-off between 12 and 14 kD was purchased from HiMedia.

2.2. Preparation of NCC from BPP. *2.2.1. Alkali Treatment.* The BPP was treated with 5% w/v NaOH at 1:50 solid to liquid ratio for removing lignin and hemicellulose. NaOH solution was taken in a beaker and then BPP was added. The solution was kept for stirring at 40 °C for 4 h at 500 rpm. The solution was filtered and the filter cake (remaining solid) was washed several times with deionized (DI) water until neutral pH has reached. The solid obtained was then kept for drying in the oven overnight at 40 °C.

2.2.2. Bleaching Treatment. Following alkali treatment, the bleaching process was performed by using 2% (w/v) sodium hypochlorite solution for 2 h at 40°C. The solid to liquid ratio was 1:10. The solution was filtered and the solid obtained was washed several times with DI water until neutral pH has reached. The obtained solid mass was kept for drying in the oven overnight at 40°C.

2.2.3. Acid Hydrolysis. The dried bleached BPP obtained from the above process was subjected to acid hydrolysis with 200 mL of sulfuric acid (55% v/v) at 50°C for 60 min. After 60 min, 10 times volume of chilled DI water was added to the suspension to quench the hydrolysis reaction. The suspension was kept overnight in the refrigerator. The supernatant was decanted and the pH of the solution was adjusted to 3 by repeated water washing followed by centrifugation at 6000*g*. In the next step, the suspension was kept for dialysis for 5−6 days in distilled water to achieve pH of 5. Finally, the suspension obtained was spray-dried and the powder was stored in the refrigerator for further use.

3. CHARACTERIZATION

BPP and spray-dried BPNCC were characterized by using different techniques such as differential scanning calorimetry, thermogravimetric analysis (TGA), attenuated total reflection (ATR)−Fourier transform infrared (FTIR), and X-ray diffraction (XRD). The morphology of BPNCC was investigated by using field emission scanning electron microscopy (FESEM) and transmission electron microscopy (TEM).

3.1. NCC Yield Calculation. The NCC yield % was calculated using the formula given below

$$\text{yield}(\%) = M_1/M_2 \times 100$$

where, M_1 = initial total weight of BPP. M_2 = dried weight of NCC samples.

3.2. ATR−FTIR Spectroscopy. BPP and NCC samples were analyzed using an ATR−FTIR spectrometer (Model: PerkinElmer 1600) to determine the functional groups of each sample in the range of 500−4000 cm^{-1} with a resolution of 4 cm^{-1}.

3.3. Morphological Features and Particle Size Analysis. *3.3.1. Particle Size and Zeta Potential Analysis.* The particle size and zeta potential of NCC measurements were determined using the Malvern Zeta sizer (Nano ZS Analyser). The NCC was diluted 100 times with DI water and sonicated for 15 min before measurement. All the measurements were taken in triplicate.

3.3.2. Field Emission Scanning Electron Microscopic Analysis. FESEM analysis was used to observe the morphological changes in NCC samples using FESEM (JEOL JSM-7000F) operated at an accelerated voltage of 10−20 kV. Before the FESEM analysis was carried out, aluminum stubs were used to mount the samples with carbon tapes and sprayed with platinum coating to avoid overcharging. The sample surface was coated with gold under vacuum before analysis. Energy-dispersive X-ray (EDX) diffraction was used for estimating the chemical composition of NCCs.[21]

3.3.3. Transmission Electron Microscopic Analysis. The morphology of NCC was examined using TEM. For TEM observation, a drop of 10 μL diluted NCC suspension was deposited on the copper grid and excess liquid was removed by

https://doi.org/10.1021/acsomega.2c06571
ACS Omega 2023, 8, 1140−1145

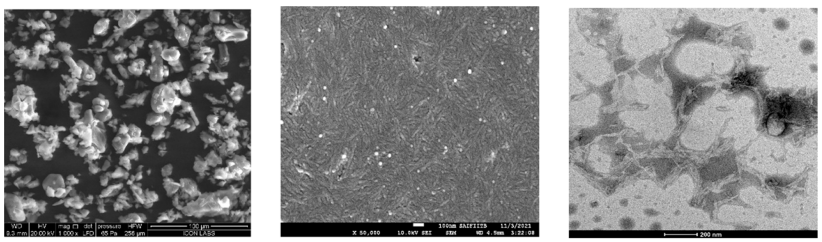

A B C

Figure 1. (A)—SEM Image of BPP, (B) SEM image of NCC, and (C) TEM image of NCC.

blotting it with filter paper after a minute and allowed to dry for 15 min. 1% wt phosphotungstic acid in water was used for the negative staining of the sample. Various particles (n = 25) were observed for the determination of average length and diameter of the NCCs.

3.4. Thermal Analysis. About 7 mg of spray-dried NCC and BPP were weighed for TGA. A differential scanning calorimeter was used for recording the thermal behavior of BPP and NCC. Thermogravimetric and derivative TGA were performed from the temperature range 30−900 °C at 20 °C min^{-1} heating rate under a nitrogen gas flowing condition.

3.5. XRD Analysis. The characterization of the degree of crystallinity of the spray-dried NCC sample was calculated by using a Shimadzu XRD-6000 X-ray diffractometer. It was operated at a voltage of 30 kV and current of 30 mA with a scanning range from 5 to 60° at a scanning speed of 2 °C/min.

The crystallinity index was calculated using

$$\text{crystallinity index, } \mathrm{CrI}(\%) = (I_{200} - I_{\mathrm{am}})/I_{200}$$

where I_{200} = crystalline peak corresponding to the intensity at approximately 22.8°. I_{am} = amorphous peak corresponding to the intensity at approximately 19.0°.

4. RESULTS AND DISCUSSION

4.1. NCC % Yield. The isolated NCC yield was found to be 29.9%. The results were compared with previously published literature. The study was carried out by Wickramasinghe et al. by extracting NCC from Sri Lankan agricultural waste by acid hydrolysis technique and the reported yield was 29%.[22] Ojumu et al. prepared NCC from cocoa pod husk (CPH) biomass waste by acid hydrolysis which showed a yield of 25%.[23] Khan et al. prepared NCC from conocarpus fiber by using the acid hydrolysis technique with maximum yield which is 19%.[24]

4.2. ATR−FTIR Spectroscopy. Infrared spectroscopy in attenuated total reflectance mode (ATR FT-IR) of BPP and NCC (Figure 3) showed a broad peak located in the range of 3450−3300 cm^{-1} which was observed in both the spectra is representative of O−H bond stretching. Compared to BPP, at 3347 cm^{-1} intense peak was observed in NCC due to hydrolysis which reflects hydrophilic properties. The peaks observed at 2919 and 2850 cm^{-1} in NCC were due to the stretching of H groups and aliphatic saturated C−H, respectively. In BPP, the peaks observed in the range of 1700−1450 cm^{-1} are assigned to the C═O stretching, C═C vibration of aromatic skeleton that shows the presence of aldehyde, carboxylic acid, and ketone in hemicellulose and lignin.[28−30] This peak is absent in NCC due to the total removal of lignin and hemicellulose. In both, the spectra of sharp and narrow bonds at 1058 cm^{-1} showed higher cellulose content due to C−O−C pyranose ring vibration. Slight changes in intensities were observed at 1452 and 1333 cm^{-1} in NCC due to the reorientation of the crystal lattice.[31] An intense peak observed at 1453 cm^{-1} in NCC is known as the crystallinity band which showed increased crystallinity degree. These results showed that the structure of NCC was intact after the hydrolysis process.[32]

4.3. Particle Size Analysis and Morphological Investigation. *4.3.1. Particle Size Analysis of NCC.* The particle size of NCC was measured in triplicate by diluting the NCC suspension with water. The particle size of NCC was found to be 209 nm and the zeta potential was −43 mV which showed good stability of the NCC suspension.

4.3.2. Morphological Investigation. The visual evaluation of different stages of manufacturing process was compared based on changes in the color. BPP was a brown color powder during alkaline treatment solution which initially changed to dark brown color and then into light yellow color during bleaching. After bleaching it is converted into pure white color which is due to the removal of wax, hemicellulose, lignin, and pectin.[25]

Microscopic evaluation, FESEM, and TEM images (Figure 1) of NCC showed needle-shaped crystals with a smooth surface compared to BPP images. The diameter and length of NCCs were found to be 16.35 ± 4.8 and 181.65 ± 24.4 nm, respectively. Similar kinds of NCC shapes reported literature are listed in Table 1.

Table 1. Dimensions of Extracted NCC Particle

materials	extraction method	length & diameter	references
NCC from calotropis procera biomass	acid hydrolysis	250 nm and 12 nm diameter	26
NCC from rice husk	acid hydrolysis	*200 nm* and 15−20 nm	27
NCC from CPH	acid hydrolysis	41−155 nm and 10−60 nm	23

Elemental analysis was conducted by using energy-dispersive XRD attached with FE-SEM. As shown in Figure 2, the EDX spectrum showed peaks for carbon and oxygen corresponding to their binding energies, respectively. The main components of NCCs are shown in Table 2 such as carbon (C K—41.67%) and oxygen (O K −58.33%). The other peaks are corresponding to the impurities which are basically due to the sulfate groups present on the surface remaining after the dialysis of NCCs.

4.4. Thermal Properties. Thermal analysis of BPP and NCC was performed to check the thermal stability of the compound. Substantial weight losses for both the materials are observed in Figure 4. DTG of the BPP sample showed three main regions of weight loss. The first degradation showed an

https://doi.org/10.1021/acsomega.2c06571
ACS Omega 2023, 8, 1140−1145

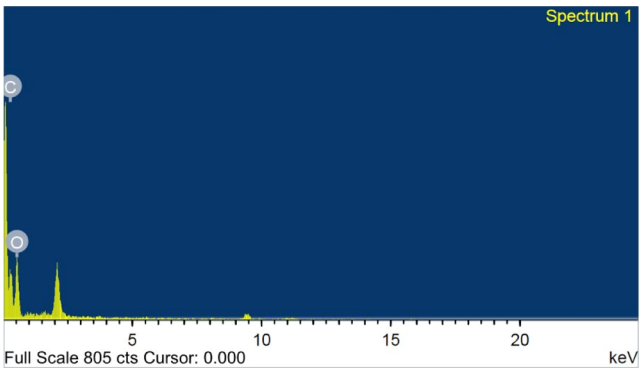

Figure 2. Energy-dispersive XRD spectrum of NCC.

Table 2. Elemental Compositions of NCC Obtained by EDX Element Weight (%) Atomic (%)

element	weight (%)	atomic (%)
C K	41.67	48.76
O K	58.33	51.24

initial weight loss below 100 °C indicated vaporization of absorbed moisture contributing to the hydrophilic character of the lignocellulose fibers. The second degradation at 278 °C, showed a sharp weight drop due to the decomposition of the glycosyl unit present in cellulose fiber, indicating the presence of hemicellulose in the chemical composition of the BPP powder.[33,34] The third degradation is around 440 °C which is probably due to higher thermal resistance of lignin content. Lignin basically used as a filler which is linked to cellulose through covalent bond helping in making cellulose denser and more stable thermally. In the NCC DTG thermogram, no extra peak was observed after 400 °C which indicated successful removal of lignin content after the hydrolysis. In the case of NCC, where a single and major degradation peak was observed at 270 °C, a similar kind of NCC thermogram was also observed by Kusmono et al.[35] As it can be seen, the amount of residue was high which is in the range of 10−40% at a temperature around 400−700 °C in BPP. This high residue showed a char fraction of BPP due to the presence of lignin and ash. A similar kind of thermogram has also been reported about the NCC prepared from rice husk which indicates high residue.[27] The two-step degradation in NCC was observed due to a higher degree of sulfonation during hydrolysis which was also indicated by the negative zeta potential of these materials. This thermal degradation is assigned to the removal of the sulfate group and further decomposition of cellulose. It can be seen in the thermogram of NCC that acid hydrolysis increases the char fraction, which is due to the introduction of the sulfated group after hydrolysis.[36]

4.5. X-ray Diffraction. XRD analysis was performed to evaluate the crystallinity of BPP and NCC, as shown in Figure 5. The XRD showed a typical cellulose Iβ structure exhibiting peaks around 16.1° (Plane 110), 22.8° (Plane 200), and 34.9° (Plane 004).[37,38] The crystallinity index obtained for NCC was 62.18% which also displayed the strongest and highest peak at 2θ = 19 and 22.2°. The increased crystallinity is due to the removal of lignin and hemicellulose after hydrolysis which caused the realignment of cellulose. During hydrolysis, the hydronium ion penetrates and promotes hydrolytic cleavage of β-1, 4-glucopyranose bonds which make it more crystalline. It was expected that an increase in crystallinity will also increase stiffness, rigidity, and therefore the strength of NCC.[27,28,39]

5. CONCLUSIONS

Extraction of NCC from BPP was successfully performed by classic treatments involving alkali, bleaching, and acid hydrolysis technique. ATR−FTIR spectra showed that hemicellulose and lignin were efficiently removed from BPP. Morphological investigation and XRD also confirmed the removal of non-cellulosic materials. The increased crystallinity index shows the removal of the amorphous part from cellulose and confirmed the formation of the crystalline structure. Acid hydrolysis is the most cost effective process for the production of NCC and it is easily practicable in industries. The process mentioned in the paper can be easily integrated into the existing process practiced by industry as the step involved

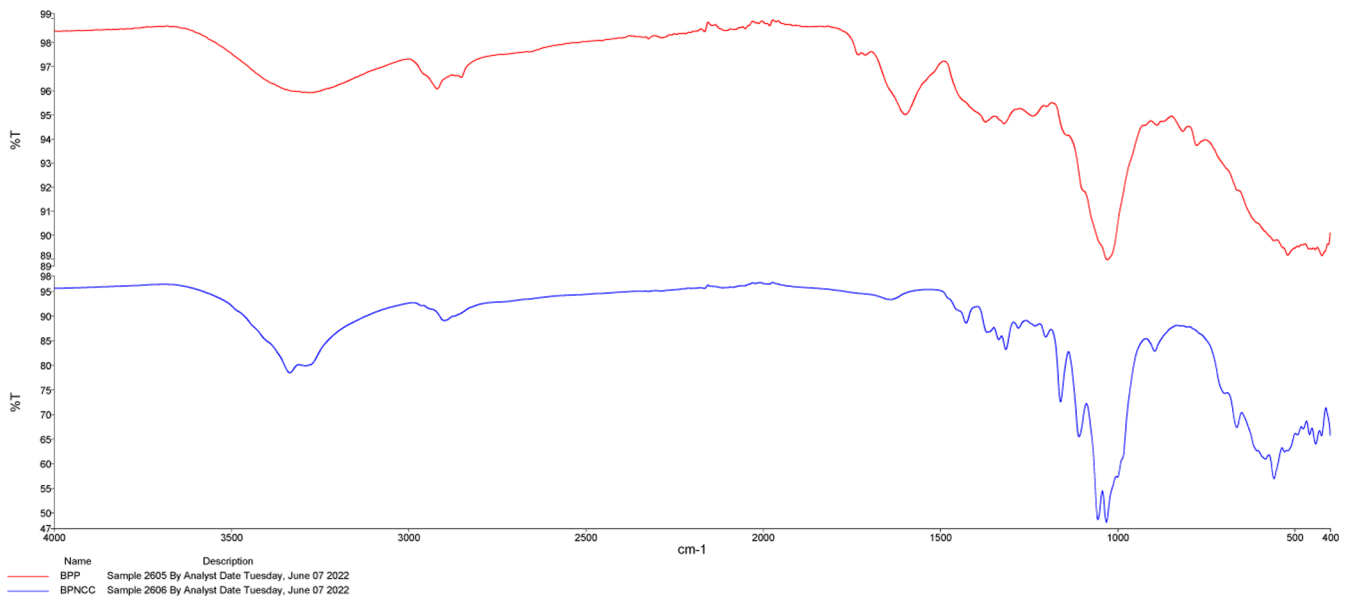

Figure 3. FTIR spectra of NCC and BPP.

https://doi.org/10.1021/acsomega.2c06571
ACS Omega 2023, 8, 1140−1145

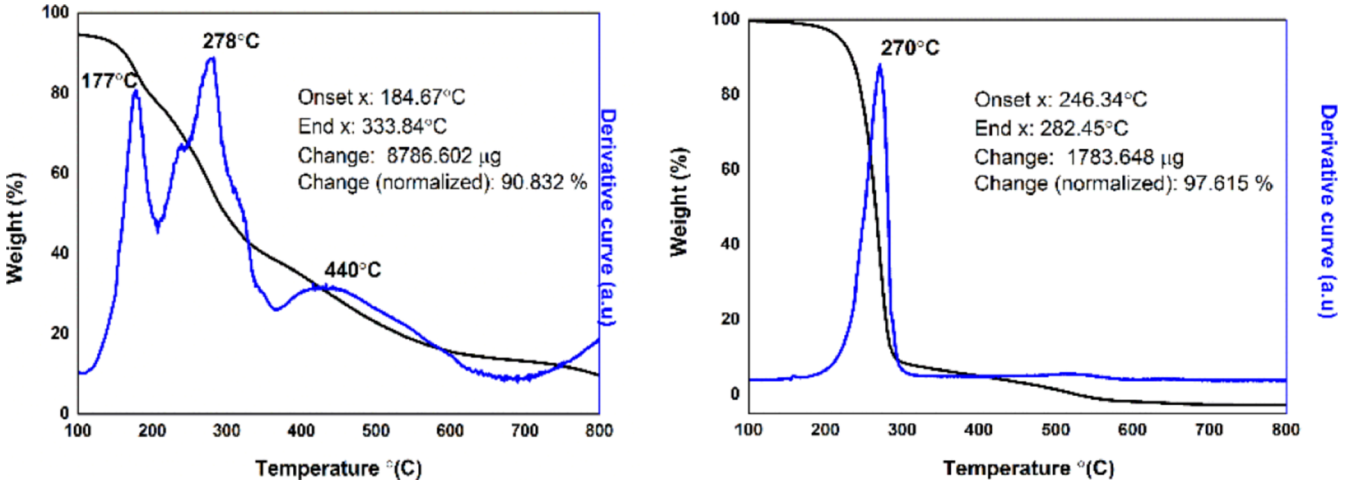

Figure 4. TGA and DTG curves of BPP (left) and NCC (right).

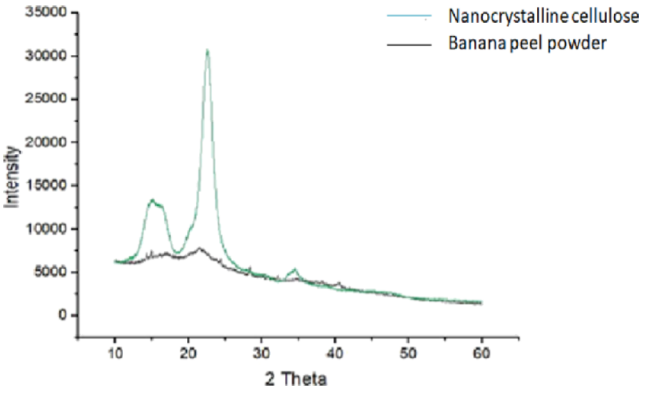

Figure 5. X-ray diffractogram of BPP and NCC.

requires minimum use of chemicals. Extracted nanocrystalline cellulose can be used as tablet excipient for oral delivery, as a main component for the nanocomposite film due to its good tensile strength, and as a conductive film in biosensors. Hence, the BP waste could be used as a good alternative for manufacturing NCC in the future.

AUTHOR INFORMATION

Corresponding Author

Bala Prabhakar − *Shobhaben Pratapbhai Patel School of Pharmacy & Technology Management, SVKM's NMIMS, Vile Parle (W), Mumbai 400056, India;* orcid.org/0000-0001-7356-4649; Email: Bala.Prabhakar@nmims.edu

Authors

Shweta Mishra − *Shobhaben Pratapbhai Patel School of Pharmacy & Technology Management, SVKM's NMIMS, Vile Parle (W), Mumbai 400056, India*

Prashant S. Kharkar − *Department of Pharmaceutical Sciences, Institute of Chemical Technology, Matunga, Mumbai 400019, India;* orcid.org/0000-0003-1955-7223

Anil M. Pethe − *Datta Meghe Institute of Medical Sciences, Wardha, Maharashtra 442004, India*

Complete contact information is available at: https://pubs.acs.org/10.1021/acsomega.2c06571

Notes

The authors declare no competing financial interest.

ACKNOWLEDGMENTS

Authors would like to thank SAIF, IIT Bombay for sample analysis.

REFERENCES

(1) Kupnik, K.; Primožič, M.; Kokol, V.; Leitgeb, M. Nanocellulose in Drug Delivery and Antimicrobially Active Materials. *Polymers* **2020**, *12*, 2825.

(2) Pathak, P. D.; Mandavgane, S. A.; Kulkarni, B. D. Fruit Peel Waste: Characterization and Its Potential Uses. *Curr. Sci.* **2017**, *113*, 444−454.

(3) Głąbska, D.; Guzek, D.; Groele, B.; Gutkowska, K. Fruit and Vegetable Intake and Mental Health in Adults: A Systematic Review. *Nutrients* **2020**, *12*, 115.

(4) Acevedo, S. A.; Carrillo, Á. J. D.; Flórez-López, E.; Grande-Tovar, C. D. Recovery of Banana Waste-Loss from Production and Processing: A Contribution to a Circular Economy. *Molecules* **2021**, *26*, 5282.

(5) Voora, V.; Larrea, C.; Bermudez, S.*Global Market Report: Bananas sustainable commodities marketplace series*, 2019.

(6) Axelos, M. A. V.; Voorde, M. H.; van de Marcel, H.*Nanotechnology in Agriculture and Food Science*; Wiley-VCH, 2017.

(7) Saravanan, N.; Sampath, P. S.; Sukantha, T. A. Extraction and Characterization of New Cellulose Fiber from the Agrowaste of Lagenaria Siceraria (Bottle Guard) Plant. *J. Adv. Chem.* **2016**, *12*, 4382−4388.

(8) Ibrahim, M. M.; El-Zawawy, W. K.; Jüttke, Y.; Koschella, A.; Heinze, T. Cellulose and Microcrystalline Cellulose from Rice Straw and Banana Plant Waste: Preparation and Characterization. *Cellulose* **2013**, *20*, 2403−2416.

(9) Padam, B. S.; Tin, H. S.; Chye, F. Y.; Abdullah, M. I. Banana By-Products: An under-Utilized Renewable Food Biomass with Great Potential. *J. Food Sci. Technol.* **2014**, *51*, 3527−3545.

(10) Lu, P.; Hsieh, Y. L. Cellulose Isolation and Core-Shell Nanostructures of Cellulose Nanocrystals from Chardonnay Grape Skins. *Carbohydr. Polym.* **2012**, *87*, 2546−2553.

(11) García, A.; Labidi, J.; Belgacem, M. N.; Bras, J. The Nanocellulose Biorefinery: Woody versus Herbaceous Agricultural Wastes for NCC Production. *Cellulose* **2017**, *24*, 693−704.

(12) Mishra, S.; Kharkar, P. S.; Pethe, A. M. Biomass and Waste Materials as Potential Sources of Nanocrystalline Cellulose: Comparative Review of Preparation Methods (2016 − Till Date). *Carbohydr. Polym.* **2019**, *207*, 418−427.

(13) Faradilla, R. H. F.; Lee, G.; Rawal, A.; Hutomo, T.; Stenzel, M. H.; Arcot, J. Nanocellulose Characteristics from the Inner and Outer Layer of Banana Pseudo-Stem Prepared by TEMPO-Mediated Oxidation. *Cellulose* **2016**, *23*, 3023−3037.
(14) Harini, K.; Ramya, K.; Sukumar, M. Extraction of Nano Cellulose Fibers from the Banana Peel and Bract for Production of Acetyl and Lauroyl Cellulose. *Carbohydr. Polym.* **2018**, *201*, 329−339.
(15) Sijabat, E. K.; Nuruddin, A.; Aditiawati, P.; Purwasasmita, B. S. S. Flat Sheet Membrane Composite for Desalinisation Applications Based on Bacterial Nanocellulose (BNC) from Banana Peel Waste, Cellulose, and Silica. *Mater. Res. Express* **2020**, *7*, 105004.
(16) Ahmad, K.; Din, Z.; Ullah, H.; Ouyang, Q.; Rani, S.; Jan, I.; Alam, M.; Rahman, Z.; Kamal, T.; Ali, S.; Khan, S. A.; Shahwar, D.; Gul, F.; Ibrahim, M.; Nawaz, T. Preparation and Characterization of Bio-Based Nanocomposites Packaging Films Reinforced with Cellulose Nanofibers from Unripe Banana Peels. *Starch—Stärke* **2022**, *74*, 2100283.
(17) Pelissari, F. M.; Andrade-Mahecha, M. M.; Sobral, P. J.; Menegalli, F. C. Nanocomposites Based on Banana Starch Reinforced with Cellulose Nanofibers Isolated from Banana Peels. *J. Colloid Interface Sci.* **2017**, *505*, 154−167.
(18) Lam, E.; Male, K. B.; Chong, J. H.; Leung, A. C. W.; Luong, J. H. T. Applications of Functionalized and Nanoparticle-Modified Nanocrystalline Cellulose. *Trends Biotechnol.* **2012**, *30*, 283−290.
(19) Tritt-Goc, J.; Jankowska, I.; Pogorzelec-Glaser, K.; Pankiewicz, R.; Ławniczak, P. Imidazole-Doped Nanocrystalline Cellulose Solid Proton Conductor: Synthesis, Thermal Properties, and Conductivity. *Cellulose* **2018**, *25*, 281−291.
(20) Zaid, M. H. M.; Abdullah, J.; Yusof, N. A.; Wasoh, H.; Sulaiman, Y.; Noh, M. F. M.; Issa, R. Reduced Graphene Oxide/TEMPO-Nanocellulose Nanohybrid-Based Electrochemical Biosensor for the Determination of Mycobacterium Tuberculosis. *J. Sens.* **2020**, *2020*, 4051474.
(21) Lee, S. Y.; Mohan, D. J.; Kang, I. A.; Doh, G. H.; Lee, S.; Han, S. O. Nanocellulose Reinforced PVA Composite Films: Effects of Acid Treatment and Filler Loading. *Fibers Polym.* **2009**, *10*, 77−82.
(22) Wickaramasinghe, W. A. W. I. C.; Lasitha, D. S.; Samarasekara, A. M. P.; Amarasinghe, D. A. S.; Karunanayake, L.Extraction and Characterization of Nano Crystalline Cellulose (NCC) from Sri Lankan Agricultural Waste. *MERCon 2019—Proceedings, 5th International Multidisciplinary Moratuwa Engineering Research Conference*; IEEE, 2019; pp 616−620.
(23) Akinjokun, A. I.; Petrik, L. F.; Ogunfowokan, A. O.; Ajao, J.; Ojumu, T. V. Isolation and Characterization of Nanocrystalline Cellulose from Cocoa Pod Husk (CPH) Biomass Wastes. *Heliyon* **2021**, *7*, No. e06680.
(24) Rasheed, M.; Jawaid, M.; Parveez, B.; Zuriyati, A.; Khan, A. Morphological, Chemical and Thermal Analysis of Cellulose Nanocrystals Extracted from Bamboo Fibre. *Int. J. Biol. Macromol.* **2020**, *160*, 183−191.
(25) Johar, N.; Ahmad, I.; Dufresne, A. Extraction, Preparation and Characterization of Cellulose Fibres and Nanocrystals from Rice Husk. *Ind. Crops Prod.* **2012**, *37*, 93−99.
(26) Song, K.; Zhu, X.; Zhu, W.; Li, X. Preparation and Characterization of Cellulose Nanocrystal Extracted from Calotropis Procera Biomass. *Bioresour. Bioprocess.* **2019**, *6*, 45.
(27) Johar, N.; Ahmad, I.; Dufresne, A. Extraction, Preparation and Characterization of Cellulose Fibres and Nanocrystals from Rice Husk. *Ind. Crops Prod.* **2012**, *37*, 93−99.
(28) Alemdar, A.; Sain, M. Isolation and Characterization of Nanofibers from Agricultural Residues - Wheat Straw and Soy Hulls. *Bioresour. Technol.* **2008**, *99*, 1664−1671.
(29) Sun, X. F.; Xu, F.; Sun, R. C.; Fowler, P.; Baird, M. S. Characteristics of Degraded Cellulose Obtained from Steam-Exploded Wheat Straw. *Carbohydr. Res.* **2005**, *340*, 97−106.
(30) Sain, M.; Panthapulakkal, S. Bioprocess Preparation of Wheat Straw Fibers and Their Characterization. *Ind. Crops Prod.* **2006**, *23*, 1−8.
(31) Kian, L. K.; Jawaid, M.; Ariffin, H.; Karim, Z. Isolation and Characterization of Nanocrystalline Cellulose from Roselle-Derived Microcrystalline Cellulose. *Int. J. Biol. Macromol.* **2018**, *114*, 54−63.
(32) Zeni, M.; Favero, D. Preparation of Microcellulose (Mcc) and Nanocellulose (Ncc) from Eucalyptus Kraft Ssp Pulp. *Polym. Sci.* **2016**, *1*, 1−5.
(33) Chen, L.; Reddy, N.; Wu, X.; Yang, Y. Thermoplastic Films from Wheat Proteins. *Ind. Crops Prod.* **2012**, *35*, 70−76.
(34) Vinayaka, D. L.; Guna, V.; Reddy, N. Ricinus Communis Plant Residues as a Source for Natural Cellulose Fibers Potentially Exploitable in Polymer Composites. *Ind. Crops Prod.* **2017**, *100*, 126−131.
(35) Kusmono, R. F.; Listyanda, M. W.; Wildan, M. N.; Ilman, M. N. Heliyon Preparation and Characterization of Cellulose Nanocrystal Extracted from Ramie Fi Bers by Sulfuric Acid Hydrolysis. *Heliyon* **2020**, *6*, No. e05486.
(36) Chen, X. Q.; Pang, G. X.; Shen, W. H.; Tong, X.; Jia, M. Y. Preparation and Characterization of the Ribbon-like Cellulose Nanocrystals by the Cellulase Enzymolysis of Cotton Pulp Fibers. *Carbohydr. Polym.* **2019**, *207*, 713−719.
(37) Nam, S.; French, A. D.; Condon, B. D.; Concha, M. Segal Crystallinity Index Revisited by the Simulation of X-Ray Diffraction Patterns of Cotton Cellulose Iβ and Cellulose II. *Carbohydr. Polym.* **2016**, *135*, 1−9.
(38) French, A. D.; Cintrón, M. S. Cellulose Polymorphy, Crystallite Size, and the Segal Crystallinity Index. *Cellulose* **2013**, *20*, 583−588.
(39) Lin, N.; Huang, J.; Chang, P. R.; Feng, L.; Yu, J. Effect of Polysaccharide Nanocrystals on Structure, Properties, and Drug Release Kinetics of Alginate-Based Microspheres. *Colloids Surf., B* **2011**, *85*, 270−279.

https://doi.org/10.1021/acsomega.2c06571
ACS Omega 2023, 8, 1140−1145